Interannual and Decadal Variability in the Tropical and Midlatitude Pacific Ocean

BENJAMIN S. GIESE

Department of Oceanography, Texas A&M University, College Station, Texas

JAMES A. CARTON

Department of Meteorology, University of Maryland at College Park, College Park, Maryland

(Manuscript received 17 September 1997, in final form 3 January 1999)

ABSTRACT

Forty-four years of mechanical and expendable bathythermograph observations are assimilated into a general circulation model of the Pacific Ocean. The model is run from 1950 through 1993 with forcing at the surface from observed monthly mean wind stress and temperature. The resulting analysis is used to describe the spatial and temporal patterns of variability at interannual and decadal periods. Interannual variability has its largest surface temperature expression in the Tropics and decadal variability has its largest surface temperature expression in the midlatitude Pacific. However, there are important interannual surface temperature changes that occur in the midlatitude Pacific and there are important decadal surface temperature changes in the Tropics.

An empirical orthogonal function (EOF) analysis of model data that has been bandpass filtered to retain energy at periods of 1–5 yr and at periods greater than 5 yr is presented. The results suggest that interannual variability is dominated by a positive feedback mechanism in the Tropics and a negative feedback mechanism in the midlatitude ocean, resulting in larger anomalies in the Tropics. A second EOF analysis of model data that has been low-pass filtered to retain periods greater than 5 yr reveals patterns of wind and surface temperature anomalies that have strikingly similar structure to the interannual patterns; however, the sequencing between the first and second EOFs is different. Even though there are large decadal anomalies of wind stress in the Tropics, the largest anomalies of surface temperature and ocean heat content occur at mid- and high latitudes. The EOF analysis indicates that decadal variability has a positive feedback mechanism that operates in the midlatitude ocean and a negative feedback mechanism that operates in the Tropics, so that the largest temperature anomalies are in midlatitudes. Previous studies have cited the contribution of heat flux anomalies as the primary cause of decadal surface temperature anomalies. These model studies indicate that meridional advection of heat is at least as important. The timing of interannual and decadal changes in the atmosphere and in the ocean suggests that the atmosphere plays an important role connecting these phenomena. One interpretation of the results is that interannual and decadal variability are manifestations of the same climate phenomena but have crucially different feedback mechanisms.

1. Introduction

The Pacific Ocean has prominent sea surface temperature (SST) variations on timescales that range from a few years to decades. This variability is often separated into two frequency bands: interannual variations with a characteristic timescale of a few years and decadal variations with a characteristic timescale of 10–20 yr. Variability at these time periods is not confined to the Pacific; recent work has shown that there are Northern Hemisphere (Mann and Park 1996) and global (White et al. 1997) modes of variability at periods ranging from a few to a hundred years. Within the Pacific basin interannual variability is dominated by El Niño–Southern Oscillation (ENSO), which has its largest signature in the Tropics, particularly the eastern tropical Pacific. This phenomenon appears primarily to be the result of interactions between the tropical oceans and overlying atmosphere (e.g., Philander 1990), and thus produces SST and heat content anomalies that are concentrated in the Tropics.

Although interannual variability has its largest SST expression in the Tropics, significant interannual variations in the North Pacific associated with ENSO events have been explored (Wallace and Gutzler 1981; Alexander 1992; Zhang et al. 1996). Interannual variability in the North Pacific is often described as the result of teleconnection patterns and has recently been described as resulting from an ''atmospheric bridge'' by Lau and Nath (1996). The atmospheric bridge operates by having the atmosphere respond quickly to SST variations in the Tropics. The resulting change in the atmospheric cir-

Corresponding author address: Dr. Benjamin S. Giese, Dept. of Oceanography, Texas A&M University, College Station, TX 77843. E-mail: giese@sweeney.tamu.edu

culation forces the midlatitude ocean, thereby linking the Tropics and extratropics through atmospheric variability. Because changes in the atmosphere are rapidly communicated to high latitude, the atmospheric bridge links the Tropics and extratropics with little time delay.

Decadal variability in the North Pacific has also been extensively documented (Trenberth and Hurrell 1994; Graham 1994). There is less of a consensus for our understanding of how anomalies grow and evolve at these low decadal frequencies. Decadal variations have been described as the result of changes in the surface latent heat, either because of reduced wind speed (Cayan 1992) or reduced air–sea temperature differences (Lau and Nath 1996). Miller et al. (1994) use a general circulation model to demonstrate that horizontal advection also contributes to changes in SST, although they found the advection term contributes about half as much as anomalous surface fluxes.

There is even less agreement on what determines the timescale of low-frequency climate variations in the Pacific. One school of thought has followed the ideas of Bjerknes (1964), who proposed that midlatitude SST anomalies result from changes in the major wind systems of the midlatitudes and their effect on ocean heat transport. In support of this point of view Latif and Barnett (1994) present a coupled atmosphere–ocean model that produces low-frequency variability with a structure similar to that observed. This perspective implies that decadal variations are internal to the midlatitudes and therefore are independent of equatorial forcing.

In contrast, Jacobs et al. (1994) propose that significant aspects of heat content variability in midlatitudes are the result of the slow propagation of waves from the tropical ocean. This point of view would suggest that the midlatitude atmosphere has little connection with, or is simply responding to, changes in the midlatitude ocean. Gu and Philander (1997) provide yet another perspective: They propose that there are decadal changes in the subduction of water in the midlatitude Pacific. When the water mass anomaly reaches the Tropics, air–sea interaction amplifies the decadal signal. Deser et al. (1996) use temperature observations to confirm the existence of decadal changes of subsurface temperature anomalies that migrate toward the Tropics; however, their analysis stops short of demonstrating that these changes alter tropical surface temperature. Lysne et al. (1997) use the results of an assimilation analysis to confirm that subsurface temperature anomalies, similar to those observed by Deser et al. (1996), do propagate to the Tropics.

The above-mentioned quasiperiodic oscillations require a time delay between the time of atmospheric forcing and the resulting decadal oceanic response. In the case of Jacobs et al. (1994) the delay results from the time that it takes for Rossby waves, excited in the Tropics by an ENSO event, to cross the Pacific and affect the dynamics of the western boundary current. The delay proposed by Gu and Philander (1997) results from the time that it takes for subducted water in the midlatitude Pacific to reach the Tropics and influence coupled ocean–atmosphere interactions there. However, there is not yet consensus on whether there is a time delay involved in decadal variability. Graham (1994), for example, describes decadal changes in the climate system during northern winter in 1976 as a low-frequency ENSO-like structure. He shows changes in SST and surface winds that occur nearly simultaneously between the Tropics and midlatitude Pacific.

Recent research has demonstrated that these two timescales of climate variability in the Pacific interact with each other. Wang (1995) and Mitchell and Wallace (1996) describe decadal changes in the timing of ENSO events and Graham (1994) describes decadal variability in the Tropics as having an ENSO-like structure.

This study examines interannual and decadal variability in the upper layers of the Pacific Ocean based on data assimilation analysis of the 44-yr period from 1950 to 1993. The analysis is based on optimum interpolation combined with a general circulation model of ocean dynamics, with a focus on the relationship between surface winds, SST, and upper-ocean heat content. Use of data assimilation provides us with a realistic estimate of midlatitude as well as tropical variability, thus allowing us to examine the relationship between these regions.

2. Historical MBT–XBT data and assimilation scheme

The bathythermograph temperature observations used in this study come from the historical compilation of hydrographic observations from the National Ocean Data Center. The dataset and the corrections that have been applied are described in detail by Levitus and Boyer (1994). In brief, the observations are checked for duplicates, for values exceeding historical ranges, and for static stability. In a few cases observations were eliminated based on subjective criteria. Finally, the observations were corrected for their systematic drop rate error, as described by Levitus and Boyer (1994).

Data distribution statistics from the mechanical and expendable bathythermograph (MBT–XBT) dataset are shown in Fig. 1. The distribution for all months from 1950 through 1993 is shown in Fig. 1a and the number of profiles from all sources is plotted as a function of depth and time in Fig. 1b (casts shallower than 25 m have been eliminated). The maximum number shown is 10 000 observations month^{-1} and the minimum number is 100. The spatial distribution (Fig. 1a) shows that the North Pacific is relatively well sampled compared to the South Pacific. The major shipping routes are clearly evident, going from North America to Hawaii and to Asia. Except for a few select routes, such as to New Zealand and along the coasts of Australia and South America, there are few observations in the South Pacific.

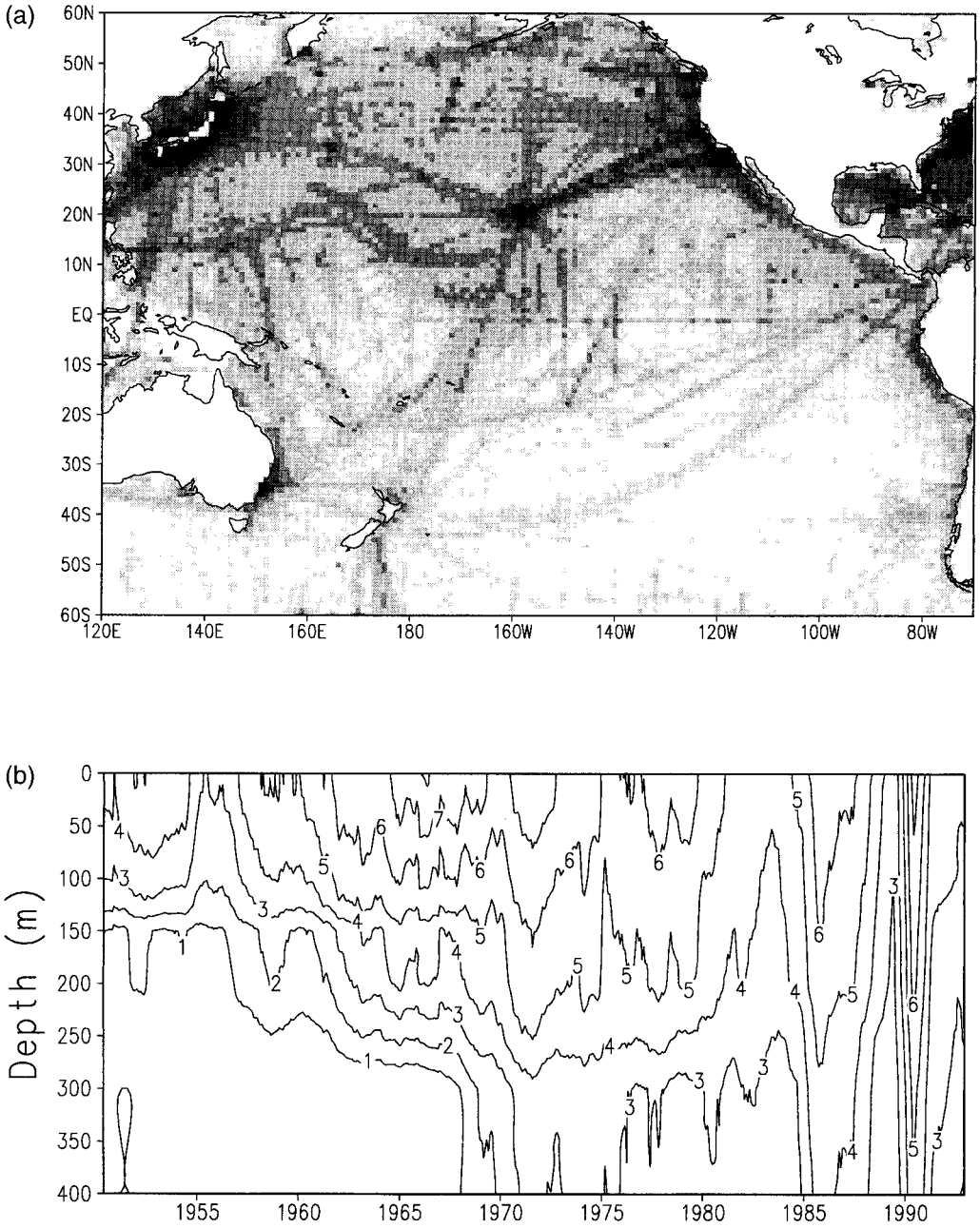

FIG. 1. Data distribution of the bathythermograph measurements. (a) Number of profiles averaged over all years. Note that the Southern Ocean has few observations relative to the Tropics and Northern Hemisphere. (b) Total number of profiles in thousands of observations per month as a function of depth and time. There is a rapid increase in number of observations below 200 m in the late 1960s when the XBT was introduced.

Because there are so few observations in the South Pacific, the analysis presented here is confined to the area 30°S–60°N. The depth distribution of observations (Fig. 1b) shows that the near-surface coverage is fairly consistent throughout the record. In contrast, the number of observations below 250 m increases dramatically in the late 1960s as a result of the replacement of the MBT with the more deeply sampling XBT.

The ocean model is based on the Geophysical Fluid Dynamics Laboratory Modular Ocean Model software. The horizontal grid resolution is 0.5° lat × 2.5° long in the Tropics, expanding poleward of 5° to a uniform 1.7° lat × 2.5° long grid at midlatitudes. The basin domain extends from 60°S to 60°N and from 120°E to 70°W. The vertical resolution is 15 m in the upper 150 m, expanding toward the deep ocean for a total of 20 vertical levels. Vertical mixing is Richardson number dependent, while horizontal diffusion and viscosity are a

constant 2×10^7 cm s^{-1}. The time step of the model is 1 h. The surface forcing conditions of wind and surface heat exchange data are provided by monthly mean surface marine observations from the Comprehensive Ocean Atmosphere Data Set (COADS) as compiled by da Silva et al. (1994).

The model employs a simple assimilation scheme that uses the MBT–XBT data and is described by Carton et al. (1996). The assimilation algorithm uses the model forecast and an update algorithm to provide corrections to the forecast. The update algorithm is based on a technique widely applied in atmospheric numerical weather prediction called optimal interpolation (Daley 1991). In optimal interpolation the differences between observed temperature and model forecast of temperature is used to update the forecast. The interpolation coefficients, otherwise known as gain matrices, are determined so as to minimize the mean square error of the analysis. Our implementation of this algorithm differs from the usual implementation because of our inclusion of spatial dependence of the assumed error statistics.

3. Results

a. Gross statistics

We begin by showing root-mean-square (rms) variability for SST anomaly from its climatological seasonal cycle in Fig. 2a and heat content from 0°-to (500-m) anomaly in Fig. 2b. Because of the lack of deep temperature observations before the late 1960s (see Fig. 1b), heat content variability is shown only for the period from 1968 through 1993. The two quantities have some interesting similarities, as well as differences. SST variability has two regions of prominent variability, a narrow band that extends from the central Pacific to the coast of South America with increasing variability toward the east, and a band of SST variability centered near 40°N and extending from the coast of Asia into the central North Pacific. In contrast with SST variability, heat content variability has its largest values in the western Pacific, with two lobes of high variability straddling the equator in the western tropical Pacific. These lobes are centered at about 8°N and 8°S and have rms values in excess of 300°C m. There is also a band of high heat content variability that is located near 40°N and extends away from the coast of Asia. Although heat content variability in the North Pacific is in the same general region as the SST variability, the two structures are not identical. While SST variability is nearly aligned with the 40° latitude and has its largest anomalies near 150°W, heat content has more pronounced north–south structure and has its largest values west of the date line. There is also some heat content variability in the eastern equatorial Pacific associated with SST variability; however, this variability is not as pronounced as the temperature signal.

In order for changes in heat storage in the ocean to affect atmospheric circulation there must be a relationship between heat storage and SST. Figure 3 shows the spatial distribution of the zero-lag correlation between these variables, computed for the period from 1968 through 1993 (when deeper temperature sampling was available). In the western tropical Pacific, where heat content variability has its largest variability, SST is largely uncorrelated with heat content, suggesting that local interaction with the atmosphere may be limited there. The regions of largest correlation (shaded areas have values greater than 0.60) are found in a 10° band of latitudes around 40°N and in the eastern Tropics. The correlation using low-pass filtered data (not shown) suggests that these basic relationships exist over a broad range of timescales.

SST and surface wind anomalies averaged from 170° to 150°W are shown in Figs. 4a,b. This longitude band captures much of the eastern Pacific temperature variability in both the Tropics and in the North Pacific. The top panel, which shows anomalous SST, demonstrates that temperature variability has both interannual and decadal timescales in the Tropics and in the midlatitudes. The tropical variability is dominated by ENSO events, which are clearly identified by warm anomalies, particularly in the years 1957–58, 1965–66, 1972–73, 1982–83, 1986–87, and 1991–92. Prominent cool periods also occur, with the largest anomalies in the years 1955–56, 1970–71, 1974–76, and 1988–89.

There is also notable decadal variability in the Tropics, although it is not as strong as the interannual variations. Equatorial temperatures are generally warmer than average after 1976 and are somewhat cooler than average in the 10-yr period just prior to 1976. This change has been described as a shift in the mean state by Graham (1994) and Trenberth and Hurrell (1994). This shift in SST is related to the simultaneous change in zonal wind stress (see Fig. 4b) on the equator from stronger than normal easterly trade winds prior to 1976 to weaker than normal easterly trade winds after 1976.

Farther west, at 160°E, decadal variability is even more pronounced. Heat content and zonal wind stress averaged from 150° to 170°E are shown as a function of latitude in Figs. 5a,b. Heat content is shown instead of SST at this section because of its large variability and because SST variability in the western Pacific is small. This section cuts through the two lobes of high heat content variability shown in Fig. 2b. The meridional structure of this variability is readily identified, with maxima at 8°–10°S and 8°–10°N. There are variations associated with particular ENSO events, with negative anomalies associated with warm events and positive anomalies associated with cold events. There is also a noticeable change in the late 1970s, when heat content anomalies at 8°S change from mostly positive to mostly negative.

The spatial and temporal structure of interannual and decadal variability is further examined by performing an empirical orthogonal function (EOF) analysis. The

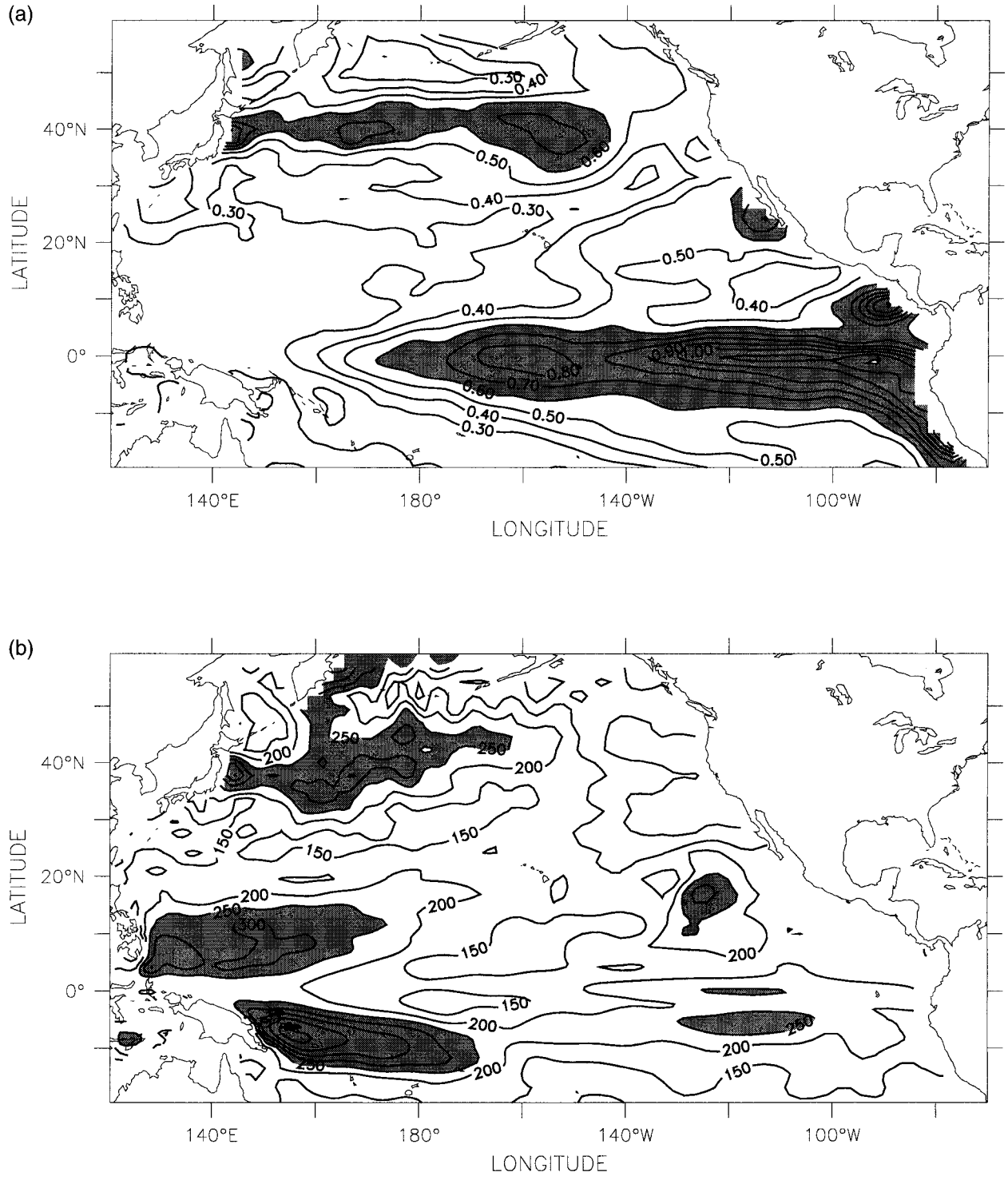

FIG. 2. Rms variability of anomalies from the annual cycle of (a) SST in °C (values greater than 0.6°C are shaded) and (b) heat content in °C m (values greater than 250°C m are shaded) for the period 1965–92.

data are initially bandpass filtered and separated into two frequency bands, interannual from 1 to 5 yr (shown in Fig. 6), and decadal from 5 to 44 yr (shown in Fig. 7). These frequency bands were chosen to separate interannual ENSO phenomena from lower-frequency phenomena. The EOFs were computed separately for each variable (SST, heat content, wind speed, and stress).

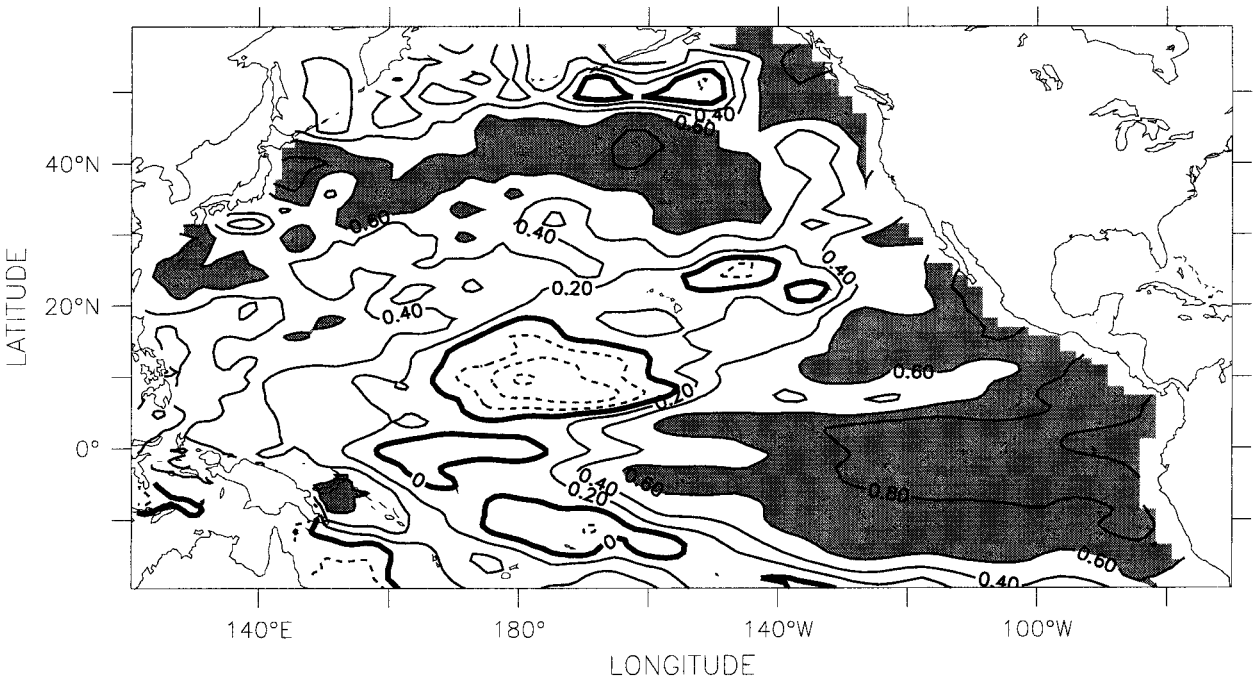

FIG. 3. Correlation between SST and heat content in the tropical Pacific from the assimilated model analysis. The annual cycle has been removed and a correlation of greater than 0.6 is shaded.

b. Interannual variability

The first EOF of interannual SST, shown in Fig. 6a, explains 60% of the variance. The amplitude of this EOF is large and positive during the El Niño events of 1957, 1972, 1982, and 1986, confirming the association of this mode with the mature phase of ENSO. Positive values of the mode are associated with warming in the central and eastern equatorial Pacific and weak cooling in the western Pacific. Interannual SST is weakly negative throughout the North Pacific with anomalies of about −0.3°C, except adjacent to the coast of North America where there are also positive anomalies.

The spatial pattern of the second interannual EOF of SST, which explains just 8% of the variance, is shown in the upper right-hand corner of Fig. 6. The second EOF shows a narrow band of positive anomaly in the central and eastern equatorial region with a maximum at 130°W. The North Pacific, in contrast with the anomaly pattern in the first EOF, has anomalies of the same sign as in the Tropics. Because the second EOF leads the first EOF (especially noticeable during the 1970s and 1980s), the pattern of anomalous SST can be interpreted as the early structure of El Niño. Tourre and White (1995) have described the relationship between the first and second EOF of SST and heat content in the Pacific Ocean and the global oceans, and identify the second EOF as a precursor mode. They use the first two EOFs to describe SST anomalies that propagate equatorially and eastward, both in the Pacific and in the Indian Oceans. Our analysis shows the first two EOFs of SST in the interannual band with a similar structure as noted by Tourre and White (1995).

In regions where heat content is highly correlated with SST, such as in the eastern equatorial Pacific and in the Kuroshio extension region, the first EOF of interannual heat content anomalies resembles the first EOF of interannual SST anomalies; that is, increases in SST are associated with increases in heat storage. The first EOF of interannual heat content, which explains 38% of the total variance, has two negative lobes in the western Tropics consistent with a redistribution of mass from west to east during El Niño. These lobes are far more prominent than in the analysis of Tourre and White (1995) (cf. their Fig. 8a). The second interannual EOF of heat content explains 16% of the variance and shows a single lobe of positive heat content anomaly that is centered on the equator in the eastern tropical Pacific. Unlike the first EOF, which has equatorially symmetric structure in the western tropical Pacific, the second EOF of heat content has structure that is distinctly south of the equator in the west. Just north of the equator, in a band from 10° to 25°N, there are negative anomalies across the entire Pacific. There is no corresponding negative SST anomaly in this band, suggesting that the decrease in heat content is due mostly to changes in the depth of the thermocline.

Near the equator the second and first EOFs of wind stress magnitude (Figs. 6k,c) and wind vectors (Figs. 6l,d) show, in that order, a progression of westerly wind anomalies moving from the western Pacific toward the

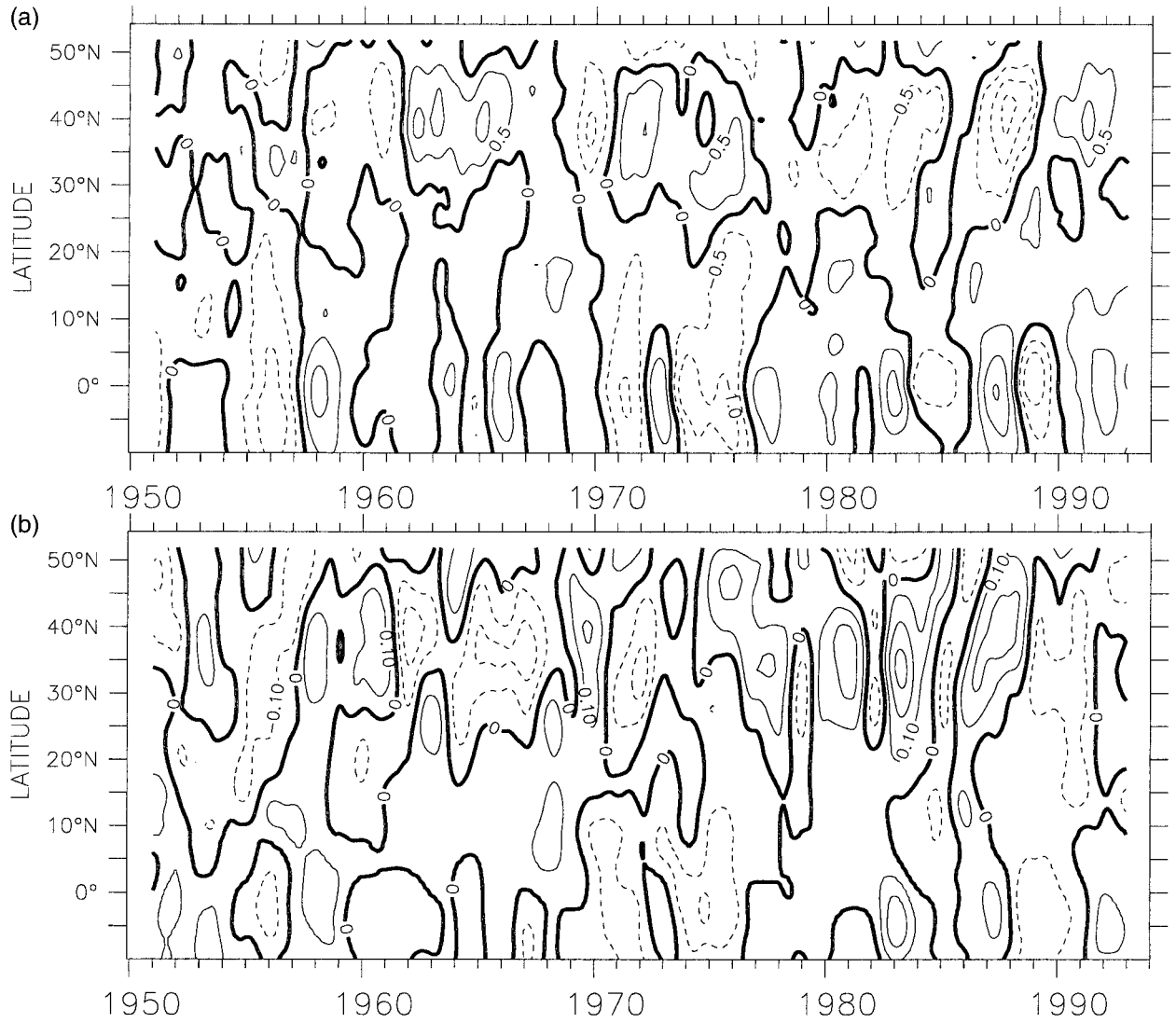

FIG. 4. Time–latitude plot of anomalous (a) SST and (b) zonal wind stress. The data have been averaged from 170° to 150°W and have been smoothed in time using a 25-month Hanning filter.

east as El Niño develops. The first EOF of wind stress magnitude (Fig. 6c) clearly shows the zonal changes on the equator, with anomalous surface convergence occurring to the west of the largest SST anomalies. Although the first EOF shows wind anomalies centered on the equator, the second EOF has an asymmetry in the anomalies across the equator. Whereas in the Tropics wind anomalies tend to be of one sign throughout the ENSO episode (sustained westerly anomalies), the anomalies reverse from being first anticyclonic during the onset phase to being cyclonic during the mature phase. Thus the second EOF has anticyclonic winds in the North Pacific coincident with warm SST anomalies preceding cyclonic winds coincident with cool SST anomalies. If the ocean directly forced the atmosphere, presumably there would be a surface low pressure over the warm SST and the circulation pattern would be cyclonic. The fact that anticyclonic winds are associated with positive SST may be evidence that the atmosphere forces the ocean in the North Pacific.

c. Decadal variability

The EOFs computed on the low-pass filtered records (>5 yr) are shown in Fig. 7. As in the case of the first two interannual EOFs, comparison of the time series for all four variables indicates that the first decadal EOF of each variable relates to the same phenomenon. The first EOF of decadal SST variability has as its most dominant structure an SST anomaly that stretches across the North Pacific from the coast of Japan to the west coast of North America. There are also SST anomalies of the opposite sign throughout the equatorial Pacific, with the largest anomalies occurring in the eastern equatorial Pacific.

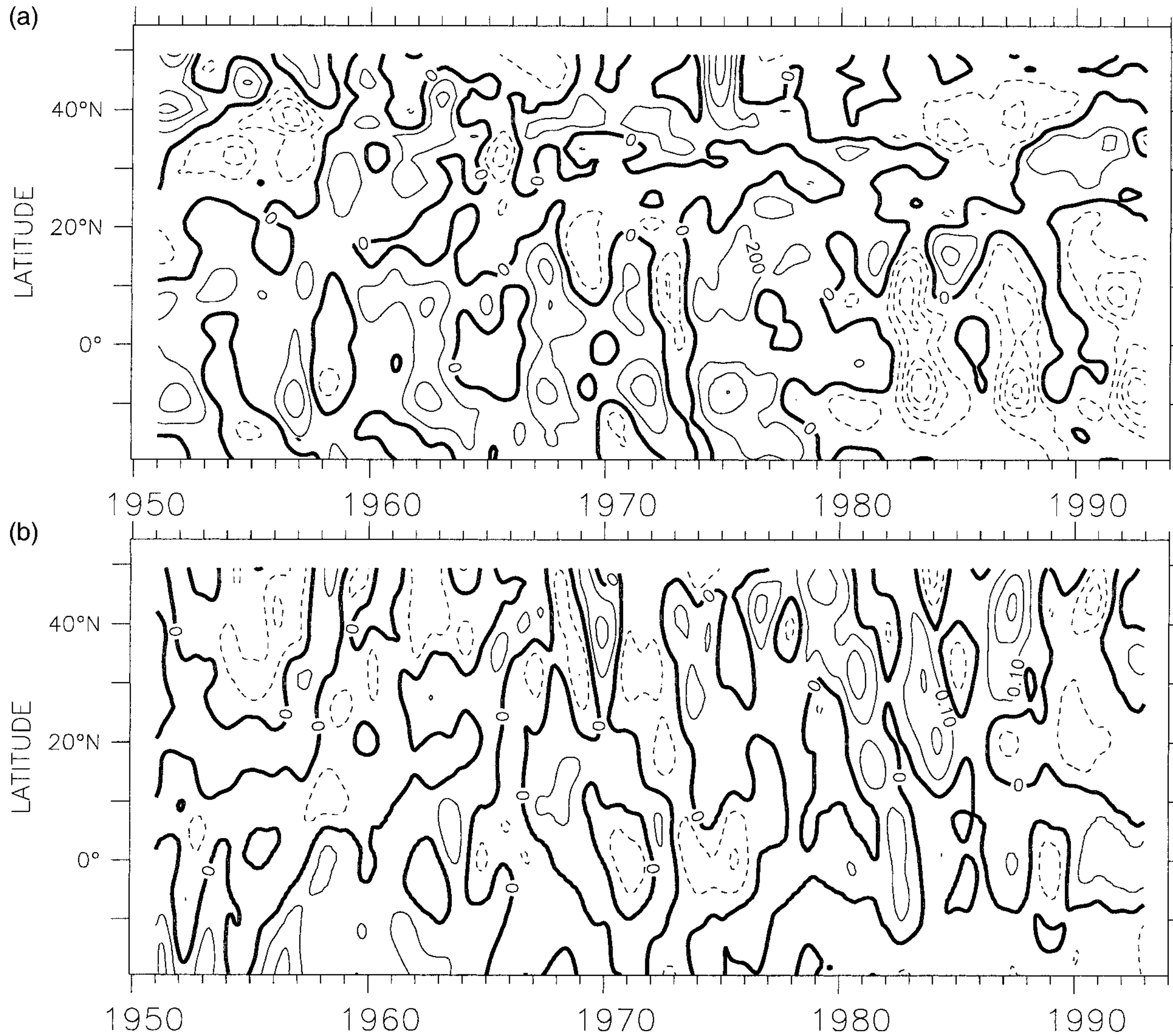

FIG. 5. Time–latitude plot of anomalous (a) heat content to 500 m and (b) zonal wind stress. The data have been averaged from 150° to 170°E and have been smoothed in time using a 25-month Hanning filter.

The time series associated with the first EOF of SST (solid line in Fig. 7e) shows that SST is anomalously warm in the midlatitudes from 1963 to 1977, changing to cooler than normal conditions during the 1980s. The Tropics have the opposite phase so that SST is cool there from 1963 to 1977, warming in the 1980s.

The first decadal EOF of heat content shows much more structure in the Tropics than the first decadal EOF of SST. There are prominent lobes of heat content anomaly that straddle the equator, with their maximum values at 10°N and 10°S. The first EOF of heat content also shows that the phase is different between the western and eastern Pacific. It is interesting to note that this mode has little signal anywhere on the equator; instead the largest heat content signal is just north and south of the equator. The time record of the EOFs of heat content show that changes in heat content lag those of SST and winds by several years.

The first EOF of the wind field also has prominent amplitude in both the Tropics and in the North Pacific. The surface wind anomalies show a pattern of cyclonic flow centered near 40°N, with the largest anomalies in the central part of the Pacific and into the Gulf of Alaska. Associated with these prominent zonal wind anomalies are negative SST anomalies centered at about 40°N.

To examine the relationship between midlatitude winds and SST we construct a midlatitude wind index, shown in Fig. 8a. The index is the negative of the average zonal wind stress at 25° and 35°N. Because the zonal wind component usually has a zero near 30°N (at the location of the subtropical high), this index has a near-zero mean. It can also be interpreted as indicating

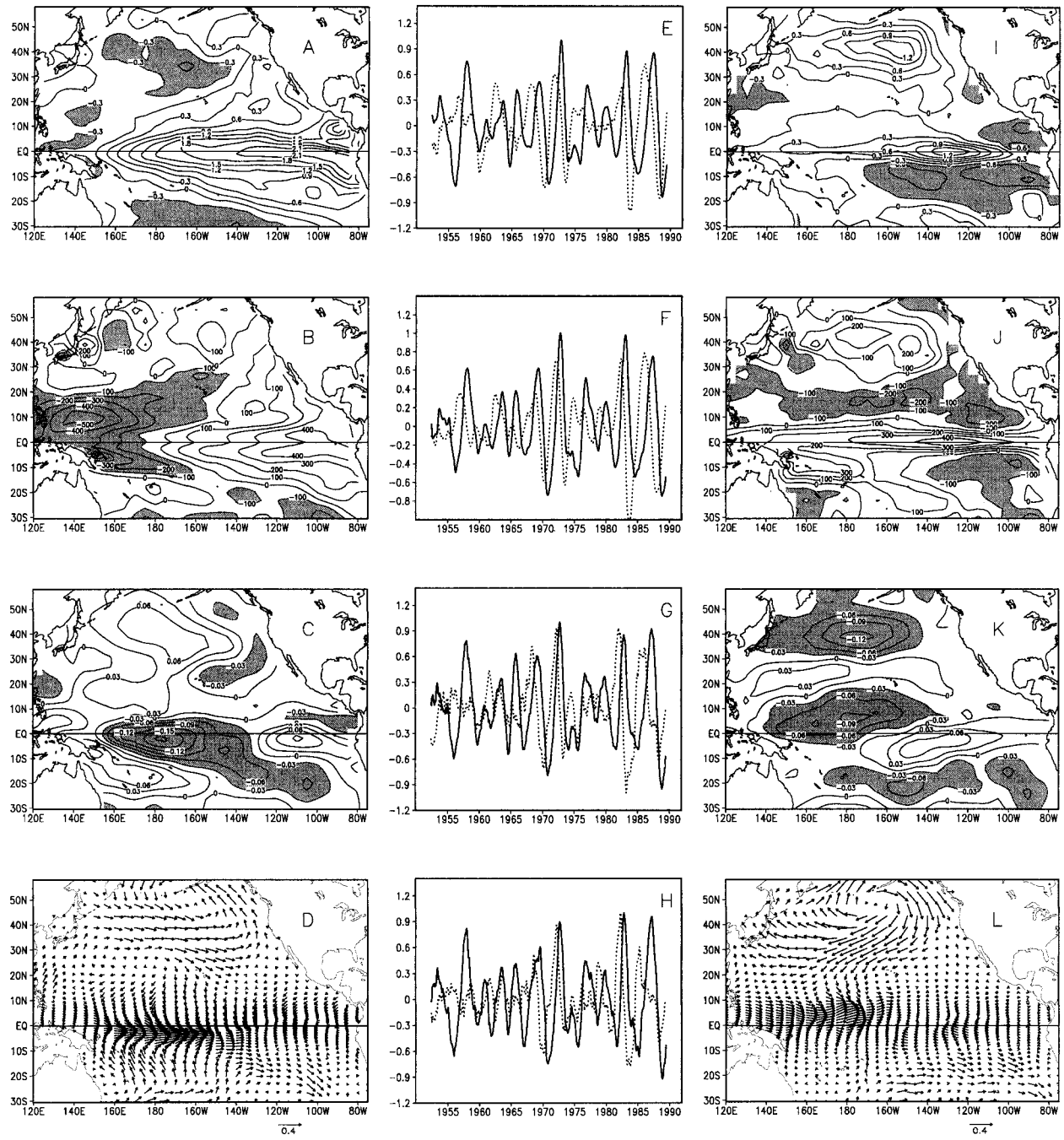

FIG. 6. Left-hand panels [(a)–(d)] show the first EOF of (a) SST, (b) heat content, (c) wind speed magnitude, and (d) vectors of zonal and meridional wind stress. The data have been bandpass filtered to retain energy with periods between 1 and 5 yr. The right-hand panels [(i)–(l)] show the second EOF for the same variables. The central panels [(e)–(h)] show the time series associated with the two EOFs, with the solid line the time series of the first EOF and the dashed line the time series of the second EOF.

the latitude of the subtropical high, with a positive value corresponding with a northward shift of the subtropical high and a negative value corresponding to a southward shift of the subtropical high. The index is mostly positive during the 1960s and early 1970s, indicating a northward displacement of the subtropical high during this period, and is largely negative during the late 1970s and 1980s, indicating a period of southward displacement of the atmospheric circulation.

Regression with the subtropical high index shows that anomalies of SST and winds are highly coherent (Fig. 8b). The association of anticyclonic flow with warm SST suggests that the atmosphere is driving the ocean response (anticyclonic winds could arguably lead to

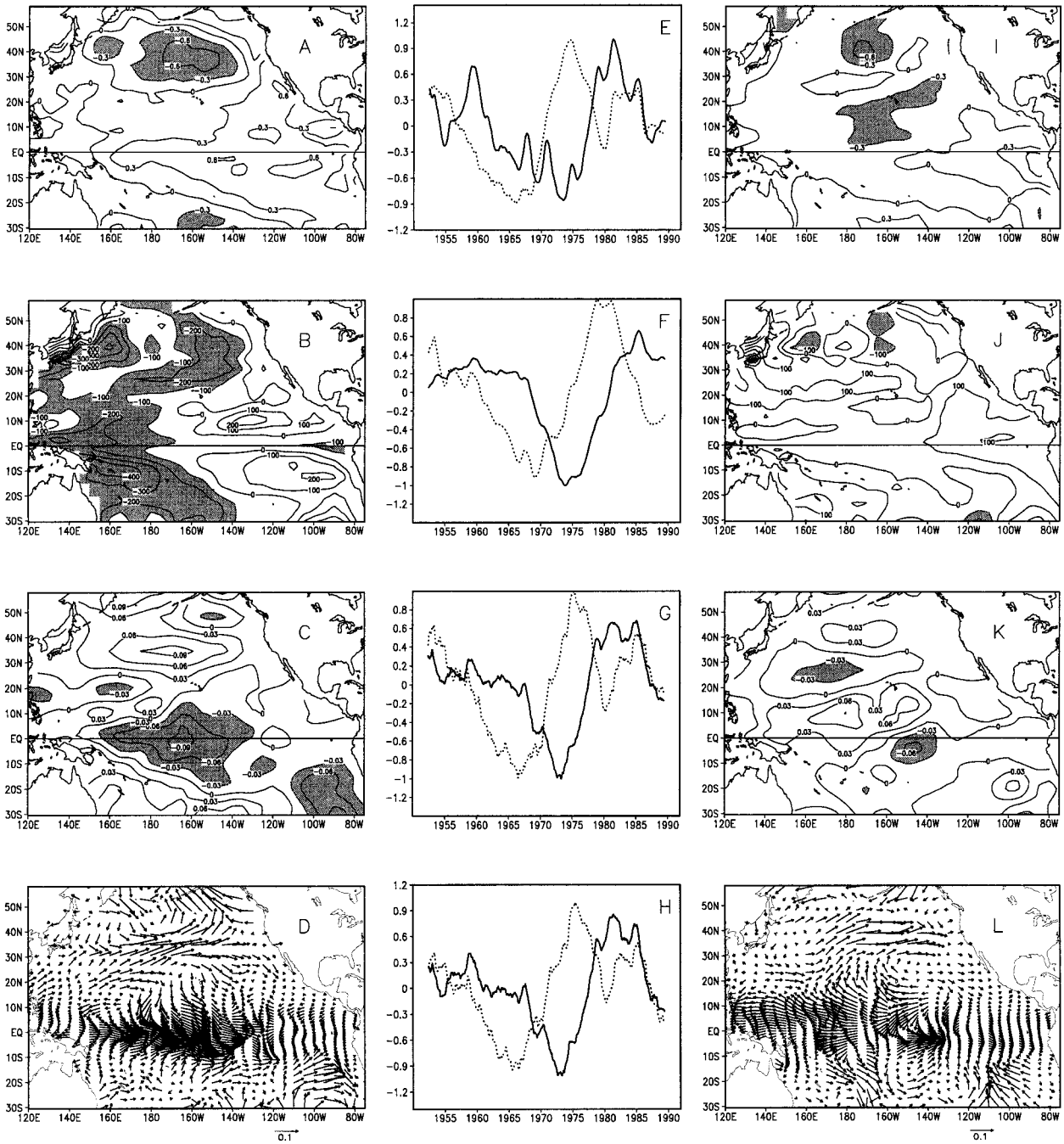

FIG. 7. As in Fig. 6, except that the data have been low-pass filtered to retain energy with periods longer than 5 yr. A linear trend was removed before low-pass filtering.

warming by downwelling, whereas a warm SST anomaly would lead to cyclonic winds). One possible explanation for the SST anomalies is that variations in wind strength cause variations in the sensible and latent heating and thus alter SST (Cayan 1992). Another possibility is that variations in wind strength cause variations in the surface currents and thereby induce SST variations by anomalous advection (Miller et al. 1994). A positive anomalous transport induced by weaker than normal westerlies will warm SST by acting against the mean meridional temperature gradient. Because the model employs Newtonian damping to observed SST, it is not possible to explicitly evaluate the relative roles of heat flux and meridional advection in the model. However, we can estimate the relative roles in the following way. The anomalous meridional advection term is contoured

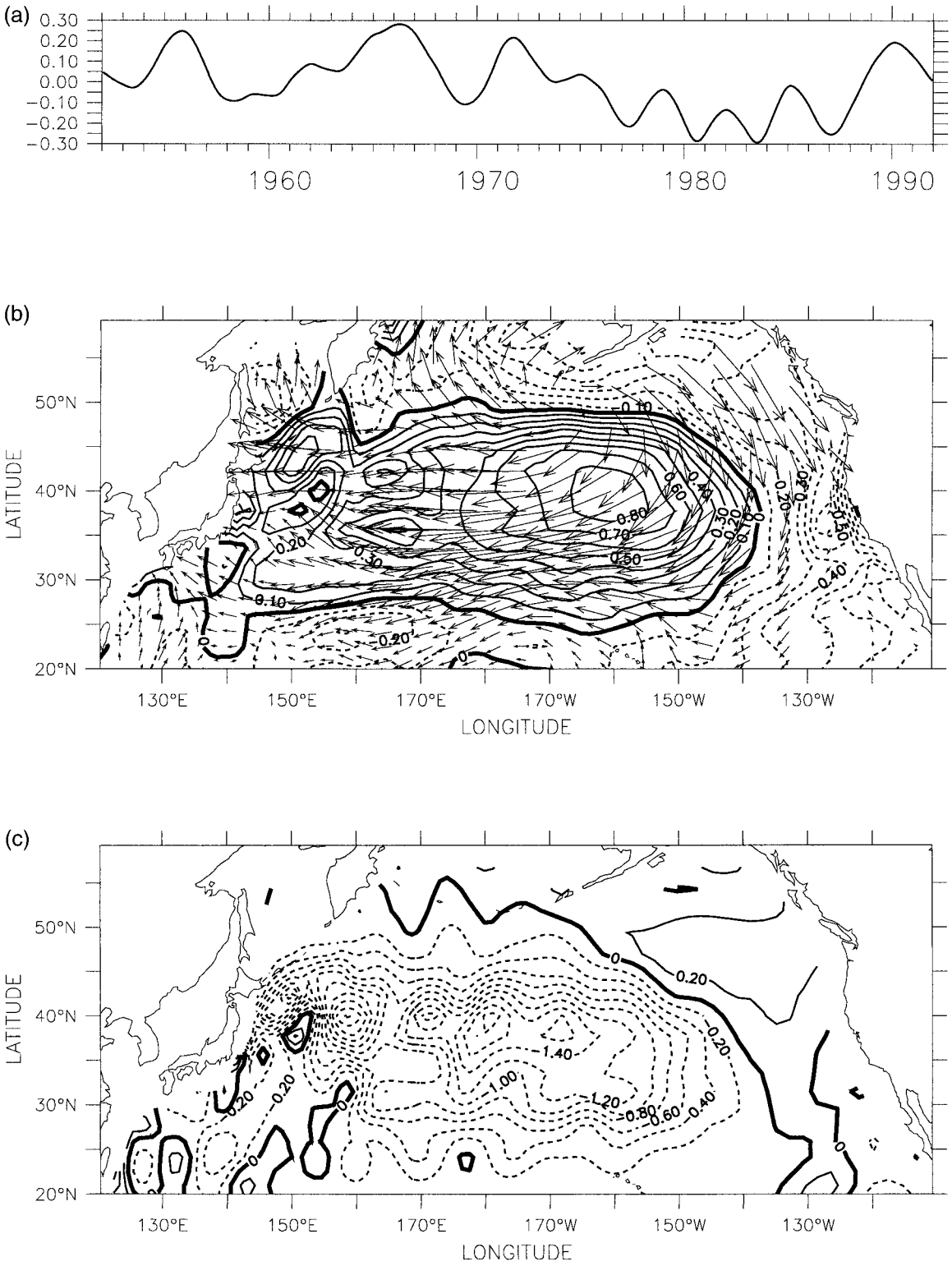

FIG. 8. Time series of the negative of zonal wind stress at 25°N plus zonal wind stress at 35°N averaged from 180° to 140°W and smoothed with a 49-month Hanning filter. This time series is used as a basis function, onto which temperature and wind stress anomalies were projected, shown in the middle panel. The bottom panel shows contours of anomalous meridional advection, also projected onto the basis function.

in Fig. 8c. If we take an average value in the heating region of -1.5×10^{-7}°C s^{-1} we get an annual heating rate of 1.5°C for a 4-month period. By way of contrast, Lau and Nath (1996) found that an 8 W m^{-2} heat flux anomaly could account for a 0.4°C over a 4-month period. Thus the heating rate in our model run is about four times larger than the heat flux term used by Lau and Nath (1996). It would appear that the decadal heat anomaly must at least result in part from the anomalous meridional advection term.

Decadal changes in SST, heat content, and winds show distinct differences between the early 1970s and the late 1970s, with a transition during 1976 (Trenberth and Hurrell 1994; Graham 1994). These differences are easily identified by comparing the anomaly fields in the decade prior to 1976 (Fig. 9) with the anomaly fields in the decade following 1976 (Fig. 10). Prior to 1976 there is anomalous anticyclonic flow throughout the North Pacific, with anomalous positive SST anomalies. In the Tropics the wind anomalies consist of stronger than normal easterly trades in the central and western Pacific, and slightly weaker than normal easterly trades in the eastern Pacific. The SST anomaly pattern has weak positive anomalies in the western Pacific and weak negative anomalies in the eastern Pacific. The anomalies of heat content in the Tropics, shown in Fig. 9b, are much more pronounced, with significant positive anomalies in the western Pacific and negative anomalies in the eastern Pacific. The anomalies in the western and eastern Pacific straddle the equator, with maximum anomalies at about 5°S and 5°N. Heat content anomalies on the equator are generally small, with weak positive values in the west and near-zero anomalies in the east. The positive heat content anomalies in the west are consistent with the presence of the stronger than normal easterly trades. The origin of the negative anomalies in the east is harder to explain: there are no substantial wind anomalies to force the heat content anomalies there. An alternative explanation is that heat content anomalies in the east are remotely forced by wind anomalies in the west.

The conditions in the 10-yr period following 1976 shows a reversal of the anomaly patterns. After 1976 SST anomalies (Fig. 10a) show a large-scale cooling of the North Pacific and a weaker warming of the eastern equatorial Pacific. Associated with the cool anomalies is a pattern of cyclonic flow in the North Pacific and weaker than normal easterlies in the central and western Pacific. Again, the eastern Pacific has an opposite wind anomaly pattern to that in the west, and the east has stronger than normal easterly trades. Heat content in the late 1970s and early 1980s (Fig. 10b) shows a response consistent with that of the positive wind stress anomalies, with lower than normal heat content associated with cyclonic flow in the west. The positive lobes in the east are not as pronounced as in the pre-1976 case, although there are positive anomalies in the east just north and just south of the equator. Again, heat content anomalies on the equator are weak across the Pacific.

4. Discussion and conclusions

In this paper we use results from a multidecadal retrospective analysis to explore interannual to decadal climate fluctuations in the tropical and North Pacific Ocean. The analysis uses MBT and XBT observations from the period 1950–93 assimilated into a general circulation model that is forced with surface wind stress and SST from COADS. The analysis shows that there is prominent interannual and decadal variability of SST, heat content, and surface wind stress in the tropical and North Pacific Ocean. SST has larger interannual variations in the Tropics and larger decadal variations in the North Pacific, even though wind stress anomalies are large in the Tropics for both timescales. An EOF analysis of the assimilation analysis shows that the leading mode of interannual variability is similar in structure to the leading mode of decadal variability with warm anomalies in the Tropics coinciding with cool anomalies in the midlatitude North Pacific, a point first made by Tanimoto et al. (1993) and subsequently confirmed by the studies of Kawamura (1994) and Zhang et al. (1997). Kawamura (1994) and Zhang et al. (1997) go on to relate decadal patterns of SST variability to large-scale changes in the atmosphere, a relationship noted by Graham (1994) in a study of an atmospheric general circulation model response to changes in SST forcing.

The EOF analysis shows that although the same basic patterns exist for the two timescales, the sequencing between the first and second EOFs is different for interannual and decadal time periods. Tourre and White (1995) were among the first to discuss the sequencing between the first and second EOFs of interannual variability, and identify the second EOF as a precursor mode to the first EOF (representing the mature phase of ENSO). Our analysis also shows the second EOF of SST distinctly leading the first EOF in the interannual band; however, the evolution of the EOFs of decadal variability differ from those of the interannual band. One interpretation for the difference in development between the interannual and decadal variability is as follows.

The progression of anomalous patterns of SST and wind between those resembling the first and second EOFs at both interannual and decadal timescales is schematicized in Fig. 11. The interannual sequence (upper panel) shows a progression from the second EOF in which there is anomalous anticyclonic wind anomalies and warm SST in the midlatitude Pacific and westerly anomalies and warm SST in the tropical Pacific (cf. Figs. 6i,l), to the first EOF, which has anomalous cyclonic flow and cool SST over the North Pacific and westerly anomalies and warm SST in the Tropics (cf. Figs. 6a,d).

We can interpret the wind anomalies in the upper left-hand corner of each diagram as the anomaly associated with a northward displacement of the atmospheric cir-

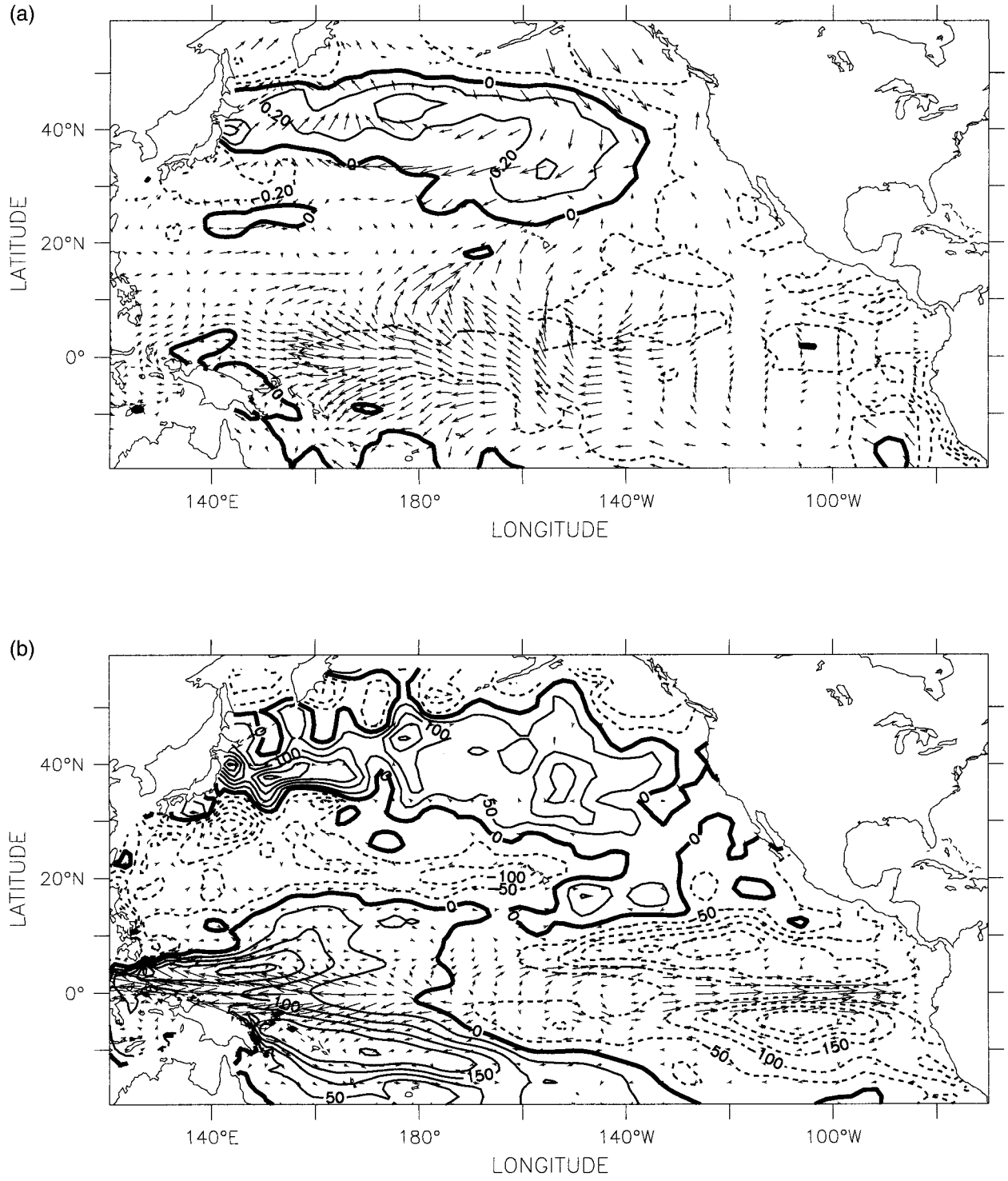

FIG. 9. (a) Contours of anomalous surface temperature and vectors of wind stress averaged over the 10-yr period from 1965 to 1975 and (b) contours of anomalous heat content and surface currents averaged from 1965 to 1975.

culation. When the winds are displaced northward anomalous westerlies develop just south of the equator to 15°N. Between 15° and 30°N anomalous easterlies develop, enhancing the existing easterly trades, while between 30° and 45°N the winds diminish in strength. Finally, the westerlies from 45° to about 55°N are enhanced while the polar easterlies become weaker north of 55°N. The result is a wind anomaly pattern much

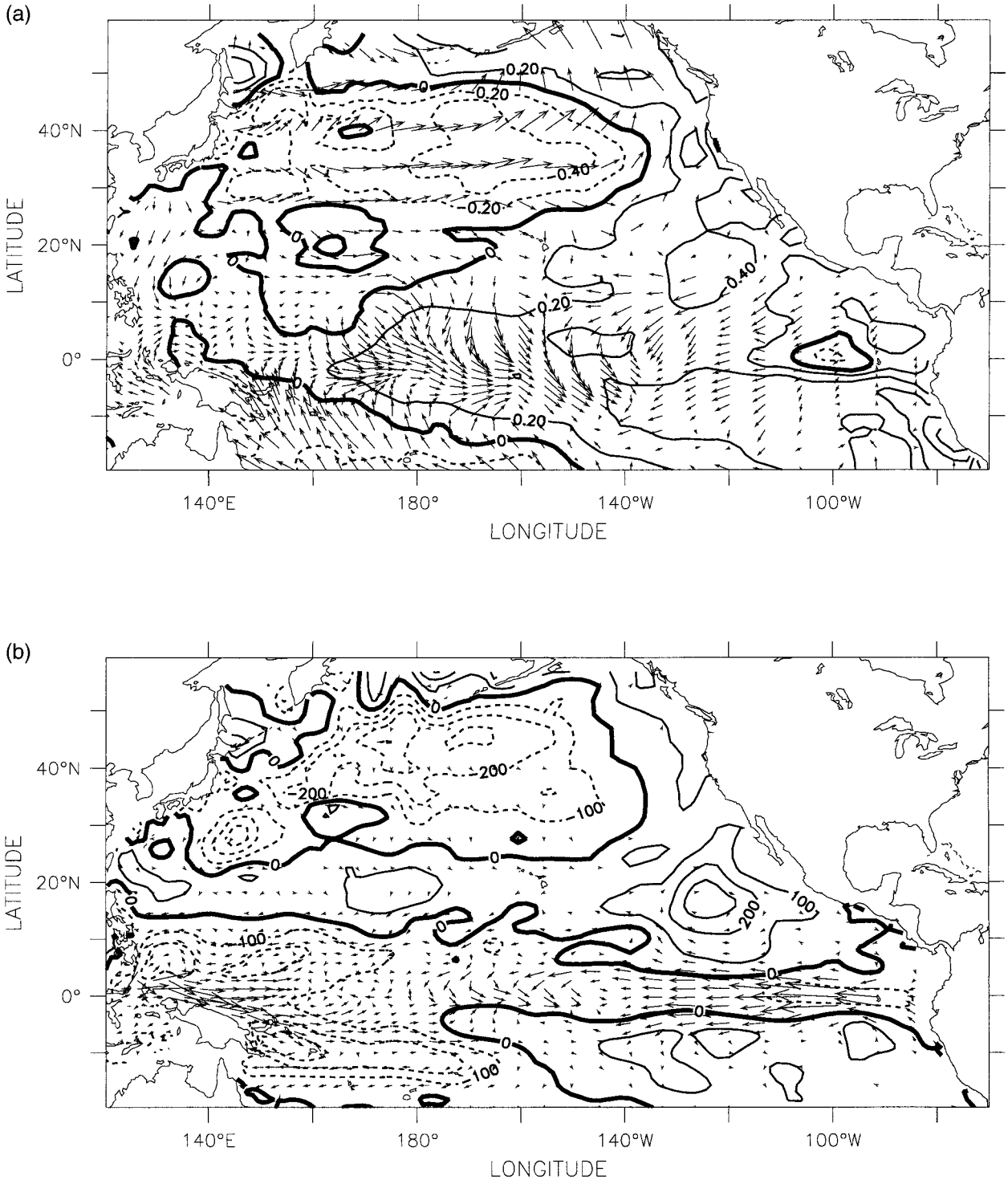

FIG. 10. As in Fig. 9, except averaged over the 10-yr period from 1977 to 1987.

like that apparent in the second EOF of interannual wind anomalies (Fig. 6l) and in the upper left-hand corner of Fig. 11.

These anomalous winds, and the related effect on latent heating, alter SST and heat content in both the equatorial region and in the North Pacific. In the Tropics, anomalous westerlies excite downwelling Kelvin waves that propagate into the eastern Pacific, where they start to warm SST and deepen the thermocline. In the North Pacific, anomalous anticyclonic flow gives rise to down-

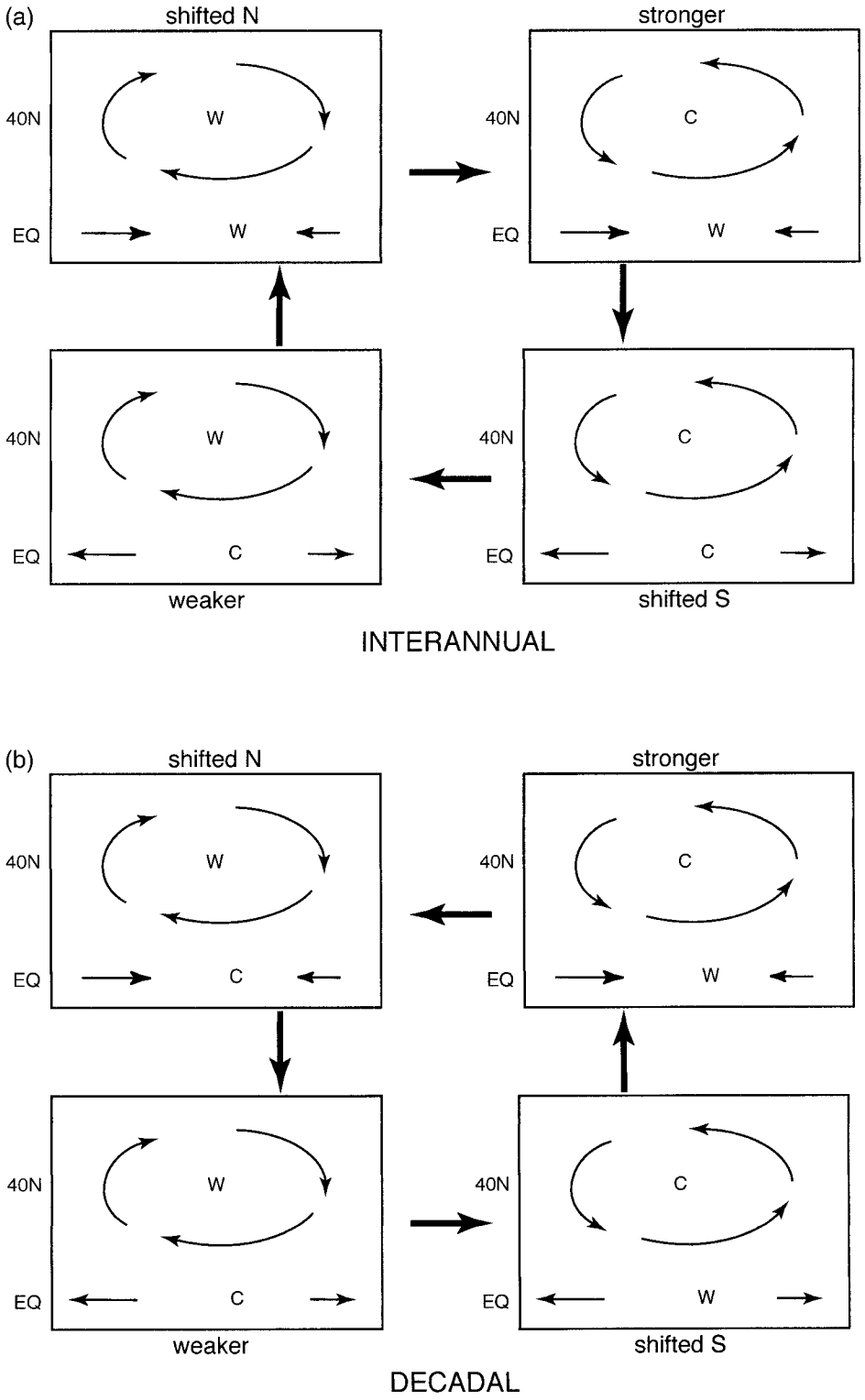

FIG. 11. Schematic diagram of the EOF patterns of SST and surface wind stress anomalies for the (a) data filtered to retain periods of 1–5 yr (cf. Fig. 6) and (b) data filtered to retain periods greater than 5 yr (cf. Fig. 7). The arrows between boxes shows the sequencing between the first and second EOFs in both cases.

welling and consequently anomalous warming of SST. The reduction of latent heating also reinforces the warm anomaly, giving rise to the positive SST anomaly shown in Fig. 6i.

The atmospheric response to positive SST anomalies is a strengthening of the atmospheric circulation, which gives strengthened westerlies from 30° to 60°N and strengthened easterlies from 30°N to near the equator. In the equatorial region, positive feedback between zonal winds and SST enhances warming of the eastern Pacific, giving rise to a sustained warm event. Thus there is continued warming in the Tropics and cooling in the North Pacific as shown in the upper right-hand panel of Fig. 11. The consequent increase in the equator-to-pole temperature gradient shifts the atmospheric circulation southward, resulting in a reversal of the wind patterns, and is shown in the lower right corner of the figure. Now there are easterly anomalies in the central equatorial Pacific and cyclonic flow in the North Pacific. These wind patterns both act to cool SST and ultimately act to weaken the atmospheric circulation.

The decadal sequence is shown in the lower panel of Fig. 11 with a progression from the second EOF (cf. Figs. 7i,l) to the first EOF (cf. Figs. 7a,d). The sequence of events at decadal timescales has the same essential patterns as at interannual timescales. However, the order is reversed. Again, consider anticyclonic winds at midlatitudes and anomalous equatorial westerlies resulting from a northward shift of the atmospheric circulation. Such a pattern is evident in the second EOF of the decadal variability during 1965. Since the positive feedback mechanisms that gave rise to growing modes in the Tropics do not exist at these lower frequencies, there are no growing warm anomalies in the Tropics. Instead, there is weak cooling in the Tropics, which, when combined with the warm anomalies in the North Pacific, gives rise to a weakened equator-to-pole temperature gradient and thus a weakened atmospheric circulation. Following the second EOF is the first EOF, which has anticyclonic flow at midlatitudes and anomalous equatorial easterlies. This pattern leads to enhanced midlatitude warming and to cooling in the Tropics. Such an anomaly pattern is clearly evident in the pre-1976 state as shown in Figs. 9a,b. The compensating effects of upwelling by the enhanced easterlies and downwelling by the reflected Rossby waves provide a negative feedback mechanism that mitigates decadal variability in the Tropics. At midlatitudes a positive feedback exists, causing a weakened meridional temperature gradient and slower atmospheric circulation, resulting in weakened midlatitude westerlies and greater warming.

The decadal winds then shift to anomalous cyclonic flow in the midlatitudes and anomalous equatorial easterlies as apparent in the early 1970s, and then to its post-1976 pattern of cyclonic flow in the midlatitudes and weaker than normal equatorial easterlies. The anomalous wind pattern gives rise to cooler temperatures in the midlatitudes and a weaker positive SST anomaly in the Tropics. Again, positive feedback strengthens the meridional SST gradient, resulting in a more vigorous circulation and enhanced cooling in midlatitudes.

Both the decadal and interannual anomaly patterns appear to result from the same basic climate phenomenon. The interannual signal is preferentially excited in the Tropics while a negative feedback exists in the midlatitudes, and the decadal signal is preferentially excited in the midlatitudes while there are negative feedbacks in the Tropics. From this perspective, ENSO is the equatorial manifestation of interannual changes in the atmospheric circulation over the entire Pacific Ocean, and decadal variability is the midlatitude manifestation of similar changes.

Acknowledgments. This work was supported by the Department of Commerce/NOAA under Grant NA26GP0472.

REFERENCES

Alexander, M. A., 1992: Midlatitude atmosphere–ocean interaction during El Niño. Part I: The North Pacific Ocean. *J. Climate,* **5,** 944–958.

Bjerknes, J., 1964: Atlantic air–sea interaction. *Advances in Geophysics,* Vol. 10, Academic Press, 1–82.

Carton, J. A., B. S. Giese, X. Cao, and L. Miller, 1996: Impact of altimeter, thermistor, and expendable bathythermograph data on retrospective analyses of the tropical Pacific Ocean. *J. Geophys. Res.,* **101,** 14 147–14 159.

Cayan, D. R., 1992: Latent and sensible heat flux anomalies over the northern oceans: The connection to monthly atmospheric circulation. *J. Climate,* **5,** 354–369.

Daley, R., 1991: *Atmospheric Data Analysis.* Cambridge University Press, 457 pp.

da Silva, A. M., C. C. Young, and S. Levitus, 1994: *Algorithms and Procedures.* Vol. 1, *Atlas of Surface Marine Data 1994,* NOAA, 83 pp.

Deser, C., M. A. Alexander, and M. S. Timlin, 1996: Upper ocean thermal variations in the North Pacific during 1970–1991. *J. Climate,* **9,** 1840–1855.

Graham, N. E., 1994: Decadal-scale climate variability in the tropical and North Pacific during the 1970s and 1980s: Observations and model results. *Climate Dyn.,* **10,** 135–162.

Gu, D., and S. G. H. Philander, 1997: Interdecadal climate fluctuations that depend on exchange between the tropics and extratropics. *Science,* **275,** 805–807.

Jacobs, G. A., H. E. Hurlburt, J. C. Kindle, E. J. Metzer, J. L. Mitchell, W. J. Teague, and A. J. Walcraft, 1994: Decade-scale trans-Pacific propagation and warming effects of an El Niño. *Nature,* **370,** 360–363.

Kawamura, R., 1994: A rotated EOF analysis of global sea surface temperature variability with interannual and interdecadal scales. *J. Phys. Oceanogr.,* **24,** 707–715.

Latif, M., and T. Barnett, 1994: Causes of decadal climate variability over the North Pacific and North America. *Science,* **266,** 634–637.

Lau, N.-C., and M. J. Nath, 1996: The role of the ''atmospheric bridge'' in linking tropical Pacific ENSO events to extratropical SST anomalies. *J. Climate,* **9,** 2036–2057.

Levitus, S., and T. Boyer, 1994: *Temperature.* Vol. 4, *World Ocean Atlas 1994, NOAA Atlas NESDIS,* 117 pp.

Lysne, J., P. Chang, and B. S. Giese, 1997: Impact of the extratropical Pacific on equatorial variability. *Geophys. Res. Lett.,* **24,** 2589–2592.

Mann, M. E., and J. Park, 1996: Joint spatiotemporal modes of surface

temperature and sea level pressure variability in the Northern Hemisphere during the last century. *J. Climate,* **9,** 2137–2162.
Miller, A. J., D. R. Cayan, T. P. Barnett, N. E. Graham, and J. M. Oberhuber, 1994: Interdecadal variability of the Pacific Ocean: Model response to observed heat flux and wind stress anomalies. *Climate Dyn.,* **9,** 287–302.
Mitchell, T. P., and J. M. Wallace, 1996: ENSO seasonality: 1950–78 versus 1979–92. *J. Climate,* **9,** 3149–3161.
Philander, S. G. H., 1990: *El Niño, La Niña, and the Southern Oscillation.* Academic Press, 289 pp.
Tanimoto, Y., N. Iwasaka, K. Hanawa, and Y. Toba, 1993: Characteristic variations of sea surface temperature with multiple time scales in the North Pacific. *J. Climate,* **6,** 1153–1160.
Tourre, Y. M., and W. B. White, 1995: ENSO signals in global upper-ocean temperature. *J. Phys. Oceanogr.,* **25,** 1317–1332.
Trenberth, K. E., and J. W. Hurrell, 1994: Decadal atmosphere–ocean variations in the Pacific. *Climate Dyn.,* **9,** 303–318.
Wallace, J. M., and D. S. Gutzler, 1981: Teleconnections in the geopotential height field during the Northern Hemisphere winter. *Mon. Wea. Rev.,* **109,** 784–812.
Wang, B., 1995: Interdecadal changes in El Niño onset in the last four decades. *J. Climate,* **8,** 267–285.
White, W. B., J. Lean, D. R. Cayan, and M. D. Dettinger, 1997: Response of global upper ocean temperature to changing solar irradiance. *J. Geophys. Res.,* **102,** 3255–3266.
Zhang, Y., J. M. Wallace, and N. Iwasaka, 1996: Is climate variability over the North Pacific a linear response to ENSO? *J. Climate,* **9,** 1468–1478.
——, ——, and D. S. Battisti, 1997: ENSO-like intedecadal variability: 1900–93. *J. Climate,* **10,** 1004–1020.